

# SURFACE MODIFICATION OF INORGANIC NANOPARTICLES USING SUPERCRITICAL SILANIZATION PROCESS

C. A. García-González<sup>1\*</sup>, A.M. López-Periago<sup>1</sup>, J. Saurina<sup>2</sup> and C. Domingo<sup>1</sup>

<sup>1</sup>Instituto de Ciencia de Materiales de Barcelona (CSIC), Campus de la UAB s/n, E-08193 Bellaterra, Spain

<sup>2</sup>Dept. of Analytical Chemistry. University of Barcelona (UB). Av. Diagonal 647 E-08028 Barcelona, Spain  
\*cgarcia@icmab.es

Nanometric titanium dioxide (TiO<sub>2</sub>) powder has been treated on the surface with octyltriethoxysilane in a supercritical carbon dioxide (scCO<sub>2</sub>) medium. The surface silanization conferred water repellency to the TiO<sub>2</sub> powder. The effect of operating variables of the supercritical silanization process (pressure, temperature) on the surface characteristics of the material was analyzed. Finally, the effect of cleaning with scCO<sub>2</sub> on the mesoporosity of the powder was studied using the principal component analysis (PCA) technique.

## INTRODUCTION

Titanium dioxide (TiO<sub>2</sub>) particles have been widely used in the industry of cosmetics because of their ability to filter and protect the skin against UV-A and UV-B lights. TiO<sub>2</sub> in the form of nanometric particles is usually chosen in order to increase the surface area for UV-protection and to avoid the whitening effect of coarser TiO<sub>2</sub> particles when rubbed on the skin.

The hydrophilic surface of the TiO<sub>2</sub> nanoparticles needs to be modified in order to increase the dispersion of the particles in nonaqueous media [1,2], as the ones used in cosmetics. Organofunctional trialkoxysilanes (RSi(OR')<sub>3</sub>), a group of non toxic and environmentally compliant chemicals, had been chosen in this work as the surface modifiers of TiO<sub>2</sub> nanoparticles. The silanization reaction [3] starts with the hydrolysis of the alkoxy groups of the silane molecules to form silanols (RSi(OR')<sub>(3-y)</sub>(OH)<sub>y</sub>). In the presence of particles with ≡OH on the surface, the silanols tend to polymerize forming a chemically attached polysiloxane network to the treated surface. Silanization could take place forming either a monolayer structure (Figure 1a) or polycondensed structures (Figure 1b), depending both on the amount of water in the medium and the type of trialkoxysilane used.



**Figure 1:** Schematic representation of (a) monolayer deposition, and (b) polycondensation.

Most of the conventional silanization methods based in the use of liquid solvents led to nanoparticles agglomeration. In the search for a more efficient process, the use of supercritical carbon dioxide (scCO<sub>2</sub>) [4] as a solvent has been envisaged as an alternative for the silanization of nanostructured materials, since scCO<sub>2</sub> is an excellent solvent for alkoxy silanes [5]. Furthermore, its properties of gaslike diffusivity and viscosity, and zero surface tension facilitate the complete wetting of the internal surface of mesoporous agglomerates of nanoparticles.

The aim of this on going research is to optimize a generic silanization method of nanoparticles using scCO<sub>2</sub> as a solvent.

## I - MATERIALS AND METHODS

### I.i - MATERIALS

TiO<sub>2</sub> nanometric particles (~ 20 nm diameter) were supplied by Degussa (P-25S). The used organosilane was octyltriethoxysilane (C<sub>8</sub>H<sub>17</sub>Si(OEt)<sub>3</sub>, Fluka). CO<sub>2</sub> (Carbueros Metálicos S.A.) was used as solvent.

### I.ii - EQUIPMENT AND PROCEDURE

The silanization of the nanometric TiO<sub>2</sub> powder was performed using the setup depicted in Figure 2. The used reactor for silanization was a 70 mL high-pressure autoclave (Thar, Re1) running in the batch mode and equipped with magnetic stirring (300 rpm) and heated using resistances (318 to 348 K). A sample of TiO<sub>2</sub> powder (~0.4 g), enclosed in cylindrical cartridges made of 0.45 μm pore filter paper, was charged on the top of the reactor. Liquid silane was added in excess (1 mL) at the bottom of the reactor. A syringe pump (Thar, P1) was used to obtain the desired operating pressure (4.9 – 22.5 ± 0.2 MPa) (see table 1). The running time was 15 - 50 min at the working pressure and temperature. Finally, the system was depressurized at ~0.8 g min<sup>-1</sup>.

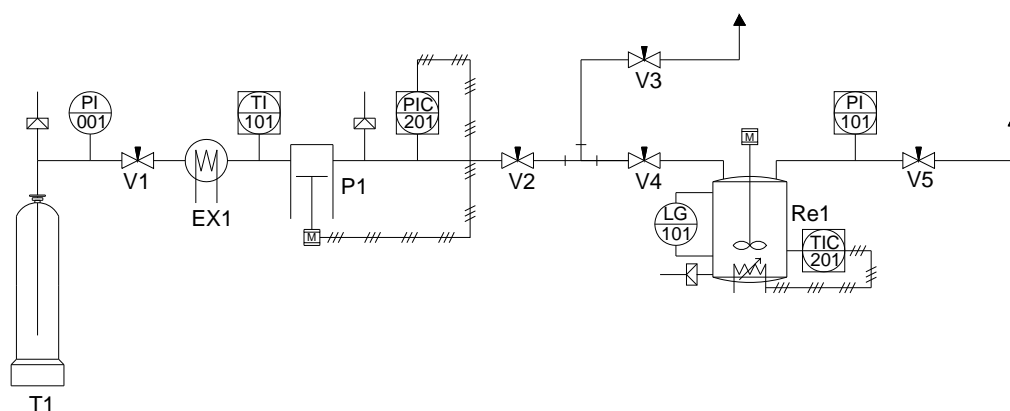


**Figure 2:** Scheme of the high pressure equipment.

The cleaning of the silanized TiO<sub>2</sub> sample was performed using a continuous flow of scCO<sub>2</sub> (2 10<sup>-3</sup>-4 10<sup>-3</sup> g min<sup>-1</sup>) at temperatures ranging from 314 to 339 K and pressures between 10.0 and 22.5 MPa during a period of time ranging from 5 to 60 min.

### I.iii - CHARACTERIZATION TECHNIQUES

Textural characteristics of raw and silanized samples were studied by low-temperature N<sub>2</sub> adsorption-desorption analysis (ASAP 2000 Micromeritics). Prior to measurements, samples were dried under reduced pressure (<1 mPa) at 393 K for 18 h. Specific surface area (*a<sub>s</sub>*) was determined by the BET method. Mean pore diameter (*D<sub>mp</sub>*), pore volume (*V<sub>p</sub>*) and total volume of pores with diameters between 10-50 Å (*V<sub>p(10-50 Å)</sub>*), 10-100 Å (*V<sub>p(10-100 Å)</sub>*), 100-1000 Å (*V<sub>p(100-1000 Å)</sub>*) and 10-1000 Å (*V<sub>p(10-1000 Å)</sub>*) were estimated using the BJH-method. Principal component analysis (PCA) was used for classifying and characterising the silanized materials produced under different experimental conditions. The algorithm was available from the “PLS\_Toolbox”, version 3.5 [6] which was implemented for use with MATLAB for Windows (Version 6.5).

## II – RESULTS

Table 1 gives the operating conditions used in this work for the silanization of the TiO<sub>2</sub> powder. In previous studies [7,8], the effectiveness of the silane coating of inorganic substrates with an alkyltriethoxysilane using scCO<sub>2</sub> as solvent has been assessed. The silane coating was thermally stable up to 500 K [8]. On the contrary, no silanization was observed in TiO<sub>2</sub> samples treated under gaseous CO<sub>2</sub> (sample T1), except when treated under near-critical conditions (sample T7).

**Table 1:** Process variables for silanized TiO<sub>2</sub> samples during 15 min.

Sample	Temperature (K)	Pressure (MPa)	CO <sub>2</sub> density (kg m <sup>-3</sup> )	H <sub>2</sub> O solubility in CO <sub>2</sub> (wt%) <sup>1</sup>
T1	318	4.9	0.106	0.15
T2	318	7.9	0.233	0.18
T3	318	8.9	0.328	0.24
T4	318	10.0	0.498	0.38
T5	318	12.4	0.674	0.58
T6	318	22.5	0.837	0.95
T7	348	5.8	0.109	0.50
T8	348	10.0	0.233	0.52
T9	348	12.2	0.328	0.62
T10	348	15.8	0.498	0.87
T11	348	17.0	0.543	0.98
T12	348	22.5	0.674	1.32

<sup>1</sup> Solubility data obtained using SUPPERTRAP v.3.1 software and PR equation of state

Results of the textural analysis showed that the nanometric TiO<sub>2</sub> primary particles form aggregates with a disordered mesoporous structure. This mesoporous character was maintained in all silanized samples. Examples are shown in Figure 3a for samples T4 and T12.

The effect of operating pressure and temperature during the silanization run, on the BET-surface area ( $a_s$ ) is depicted in Figure 3b. At low pressures, the  $a_s$  decreased when increasing the working pressure, due to the increase of silane solubility in scCO<sub>2</sub> coupled with the low solubility of water in scCO<sub>2</sub> (Table 1). In these cases, silane polycondensation (Figure 1b) could not be avoided and led to the blockage of the small pores, resulting on a decrease of BET-surface area (Figure 4). On the other hand, for total silane solubilisation, observed at  $P > 10.0$  MPa and 12.2 MPa for T of 318 K and 348 K, respectively, the  $a_s$  increased as the pressure increased. In these cases, the CO<sub>2</sub> density increases with pressure (Table 1), leading to a decrease of the silane concentration in the supercritical medium. Hence,  $a_s$  for silanized TiO<sub>2</sub> was higher at 318 K than at 348 K for the same value of pressure because of its higher density at 318 K (Table 1).

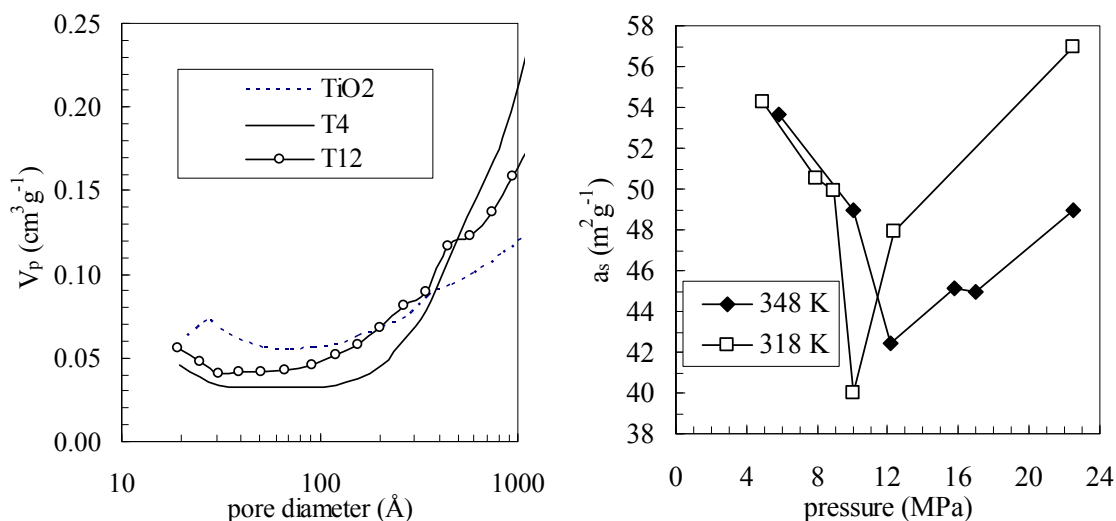


**Figure 3:** (a) Pore volume distribution of raw and silanized TiO<sub>2</sub>; (b) effect of pressure on supercritical silanization process

PCA was used for obtaining a general mapping of silanized samples under several experimental conditions in order to investigate analogies, differences, clusters, etc. and correlations between variables. Data used for PCA study corresponded to the 6 main parameters obtained in the textural analysis (Table 2). Prior to PCA treatment, data were autoscaled to provide similar weights to these 6 parameters.

**Table 2:** Parameters used for PCA analysis

Parameter	Description
$D_{mp}$	Mean pore diameter ( $\text{\AA}$ )
$a_s$	BET- surface area ( $\text{m}^2\text{g}^{-1}$ )
$V_{p(10-50 \text{ \AA})}$	Total volume of pores with diameter between 10 and 50 $\text{\AA}$ ( $\text{cm}^3\text{g}^{-1}$ )
$V_{p(10-100 \text{ \AA})}$	Total volume of pores with diameter between 10 and 100 $\text{\AA}$ ( $\text{cm}^3\text{g}^{-1}$ )
$V_{p(10-1000 \text{ \AA})}$	Total volume of pores with diameter between 10 and 1000 $\text{\AA}$ ( $\text{cm}^3\text{g}^{-1}$ )
$V_{p(100-1000 \text{ \AA})}$	Total volume of pores with diameter between 100 and 1000 $\text{\AA}$ ( $\text{cm}^3\text{g}^{-1}$ )

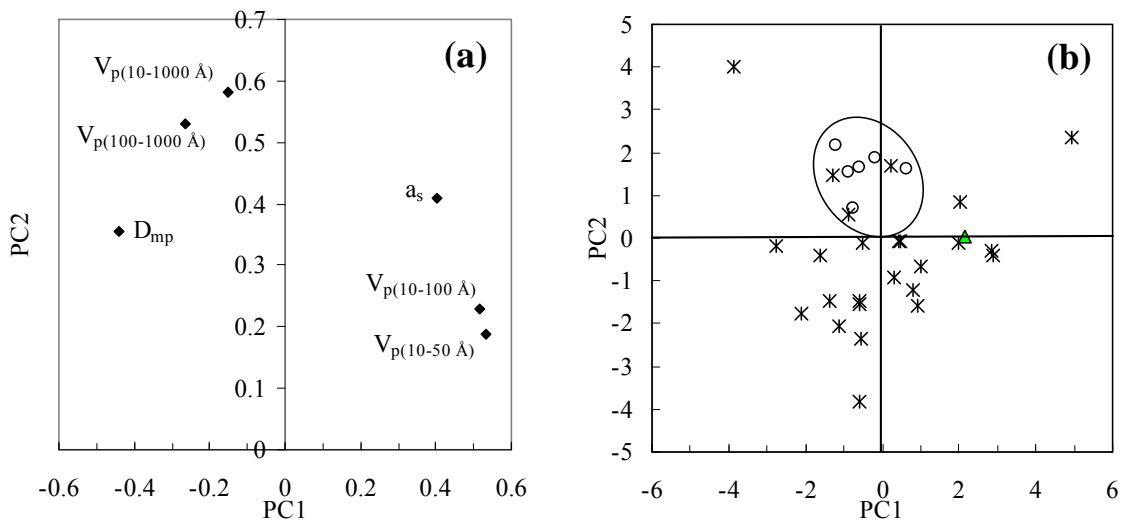


**Figure 4:** PCA result. (a) Loadings plot, and (b) scores plot: (triangle) sample uncleaned; (○) sample cleaned with  $\text{scCO}_2$  flow; and (\*) rest of samples.

The study of the variance explained by each principal component (PC) showed that 2 factors were sufficient to retain a 98% of the total information of the system. Hence, plots involving PC1 and PC2 managed to describe the behavior of the whole system. Figure 4a shows scatter plots of scores and loadings of PC1 and PC2. Loadings indicated that  $a_s$  and  $D_{mp}$ , mainly influenced on PC1. Conversely, pore volume variables defined the PC2 as they were at the top and bottom of the graph. This picture was in agreement with preliminary correlation results, as those variables correlating positively appeared in close positions while those variables cavorting negatively were in the opposite sides of the component. As a conclusion, there was a noticeable co-variation among  $a_s$ ,  $V_{p(10-50 \text{ \AA})}$  and  $V_{p(10-100 \text{ \AA})}$  due to the important contribution of small pores to the surface area. Analogously,  $V_{p(10-1000 \text{ \AA})}$ ,  $V_{p(100-1000 \text{ \AA})}$  and  $D_{mp}$ , also co-varied because of the effect of the presence of big pores on total pore volume and mean pore diameter. Figure 4b depicts the distribution of the  $\text{TiO}_2$  samples on PC1 and PC2, where those samples lying to the right of the graph presented high  $a_s$  values and low  $D_{mp}$ , and *vice versa*. As a general description of the behavior on PC2, samples with the highest percentages of small pores were at the bottom and those with a predominance of big pores were at the top of the graph.

Following, the influence of operational variables such as cleaning step, density, reaction time and depressurization rate on the distribution of samples was estimated. Among them, the effect of cleaning the silanized samples with a flow of  $\text{scCO}_2$  on sample porosity was found to be significant. As shown in Figure 4b, cleaned samples were in a well-defined cluster in the centre of PC1 and top of PC2. Specifically, a sample (triangle) was supercritically silanized at 348 K and

10.0 MPa during 50 min and subsequently cleaned with a continuous scCO<sub>2</sub> flow under different operating temperatures and pressures. Points corresponding to supercritically cleaned samples (circles in Figure 4b) were clustered in a different region of the abstract space defined by the PC's than the uncleaned sample (triangle). The differential behavior in porosity of the samples after cleaning was, thus, demonstrated. A simultaneous look at the loading and score plots of Figure 4 allowed to see that the fractionation pattern of  $V_{p(10-1000 \text{ \AA})}$ , and  $V_{p(100-1000 \text{ \AA})}$  were strongly correlated with the supercritical cleaning process. Hence, there was an important appearance of big pores in the structure of the silanized TiO<sub>2</sub> samples likely due to the channeling induced by the flow of scCO<sub>2</sub>.

Finally, a preliminary test on the hydrophobic behavior of the silanized material was performed by placing a water droplet on the surface of pellets of compacted TiO<sub>2</sub> powder and silanized afterward, using similar reaction conditions than for T8 sample. It was observed that for the pellet of untreated TiO<sub>2</sub>, the contacting angle of water was initially less than 30° (Figure 5a) indicating a hydrophilic material. On the contrary, for the silanized pellet, the water droplet on the top of the surface had a contact angle greater than 90° (Figure 5b) showing its hydrophobic character.

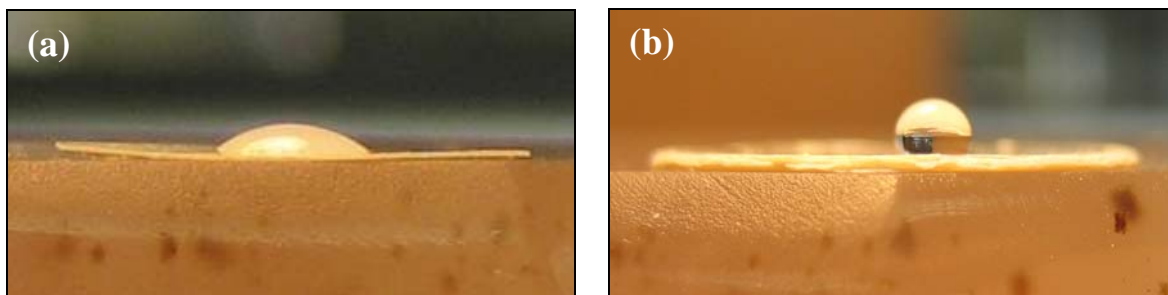


**Figure 5:** Water droplet over pellets of (a) untreated, and (b) silanized TiO<sub>2</sub> samples.

## CONCLUSION

The influence of different experimental variables on the surface treatment of nanometric inorganic particles of TiO<sub>2</sub> using a supercritical silanization method was presented. The silane concentration in the scCO<sub>2</sub> medium during the reaction played an important role on the textural characteristics of the silanized TiO<sub>2</sub> samples. Changes in operating pressure and temperature were used to tune the silane concentration in scCO<sub>2</sub> leading to a silanized material with small changes in the surface area and porosity with respect to the raw TiO<sub>2</sub>. The cleaning of the surface treated samples with a continuous flow of scCO<sub>2</sub> led to pore opening and a decrease in the surface area. Finally, the long-chain alkyl group of the used silane conferred hydrophobicity to the treated samples.

## ACKNOWLEDGMENTS

The financial support of EU Project STRP SurfaceT NMP2-CT-2005-013524 and the Spanish MEC projects (MAT2005-25567-E, MAT2005-25503-E and MAT2006-28189-E) are greatly acknowledged. C. A. García-González and A. M. López-Periago give acknowledgment to CSIC for its funding support through I3P fellowships.

## REFERENCES

- [1] LIN, Y.-L., WANG, T.-J., JIN, Y., Powder Technology, Vol. 123, **2002**, p. 194.
- [2] WANG, Z.-W., WANG, T.-J., WANG, Z.-W., JIN, Y., Powder Technology, Vol. 139, **2004**, p. 148.
- [3] PLUEDDEMANN, E.P., Progress in Organic Coatings, Vol. 11, **1983**, p. 297.
- [4] SUN, Y., Supercritical Fluid Technology in Materials Science and Engineering. Marcel Dekker (Ed.), **2002**.

- [5] DOMINGO, C., LOSTE, E., FRAILE, J., The Journal of Supercritical Fluids, Vol. 37, **2006**, p. 72.
- [6] WISE, B.M., GALLAGHER, N.B., BRO, R., SHAVER, J.M., WINDIG, W., KOCH, R.S., PLS Toolbox, Version 3.5 for use with Matlab. Eigenvector Research (Ed.), **2005**.
- [7] GARCÍA-GONZÁLEZ, C.A., ANDANSON, J.-M., KAZARIAN, S.G., SAURINA, J., DOMINGO, C., Proceeding of Eurofillers 2007, Zalakaros (Hungary), **2007**.
- [8] GARCÍA-GONZÁLEZ, C.A., SAURINA, J., DOMINGO, C., Proceeding of 5th Int. Simp. on High Pressure Processes Tech. and Chem. Eng., Segovia (Spain), **2007**.